

# Mode-selective photoisomerization in 5-hydroxytropolone. II. Theory

John J. Nash and Timothy S. Zwier<sup>a)</sup>

Department of Chemistry, Purdue University, West Lafayette, Indiana 47907-1393

Kenneth D. Jordan<sup>a)</sup>

Department of Chemistry, University of Pittsburgh, Pittsburgh, Pennsylvania 15260

(Received 7 October 1994; accepted 20 December 1994)

*Ab initio* calculations are used to explore the ground-state potential energy surface for the *syn-anti* photoisomerization reaction of 5-hydroxytropolone (5-HOTrOH). Two reaction coordinates are identified, involving 2-OH tunneling and 5-OH torsion. Hartree-Fock (HF) and perturbation theory (at the MP2 level) have been used to calculate the stationary points on the two-dimensional surface associated with these coordinates. Similar calculations on the parent molecule tropolone are carried out for comparison. As observed in previous studies, the 2-OH tunneling barrier drops dramatically at the MP2 level which includes electron correlation. Vibrational frequency calculations are carried out for both tropolone and 5-HOTrOH at the HF/6-31G\*\* and MP2/6-31G\*\* levels in order to correlate the modes with those observed experimentally. A method is introduced for evaluating which normal coordinates should be most strongly coupled to a given reaction coordinate. Normalized, mass-weighted intrinsic and direct reaction coordinates similar in form to the normal coordinates are devised by projecting atomic displacements from the reactant structure toward a transition state (intrinsic) or product (direct) structure. These serve as limiting cases for the initial projections of the multidimensional reaction trajectories. The intrinsic and direct reaction coordinates are then expanded in the basis set of normal coordinates to obtain coefficients of expansion of the reaction coordinates in this basis set. This simple scheme highlights the subset of normal coordinates which are important in promoting reaction by H-atom tunneling or O-H torsion. In 5-HOTrOH, an in-plane mode calculated at  $348\text{ cm}^{-1}$  has a large coefficient of expansion along both intrinsic and direct reaction coordinates. This mode is assigned as the "promoter mode" W observed in the experimental study of paper I. © 1995 American Institute of Physics.

## I. INTRODUCTION

The experimental work on 5-hydroxytropolone (5-HOTrOH) presented in the preceding paper (paper I) has demonstrated high vibrational mode selectivity in the  $S_0-S_1$  *syn-anti* photoisomerization of 5-HOTrOH. One of the most important deductions of that study is the identification of a "promoter mode" (denoted W in paper I) which appears to be especially important in enhancing *syn-anti* coupling in the  $S_1$  state. This in-plane mode is highly Franck-Condon active and is correlated with a vibrational frequency of  $336\text{ cm}^{-1}$  in the *syn* and  $337\text{ cm}^{-1}$  in the *anti* ground-state wells.

What is lacking in the experimental study is direct insight into the nature of this vibrational mode. In particular, we seek a further understanding of why this mode is particularly suited to promote the *syn-anti* isomerization. Similar questions can be raised about the vibrational mode specificity of the H-atom tunneling splittings observed in the symmetric parent tropolone.<sup>1-4</sup>

Much previous work on intramolecular H-atom tunneling has focused attention on a few spatial coordinates which play key roles in the H-atom tunneling.<sup>5-15</sup> Not surprisingly, these coordinates (e.g., the O-O distance) typically are localized in the vicinity of the tunneling hydrogen atom. Such descriptions have successfully accounted for the magnitude of the tunneling splitting in model polyatomics such as malonaldehyde.<sup>5</sup> They have also demonstrated that heavy

atom motion plays a decisive role in determining the rate of H-atom tunneling.<sup>5,14</sup> However, energy levels calculated in the 2D and 3D potential energy surfaces do not project in a straightforward way onto the vibrational levels of the molecule,<sup>5</sup> as one would wish in addressing questions of vibrational mode selectivity in the tunneling reaction.

In order to identify the promoter mode in 5-HOTrOH, we seek a measure of the effectiveness of each vibrational mode in taking the molecule along the tunneling reaction coordinate. To that end, Sec. II reports *ab initio* calculations of the structures, normal modes, and vibrational frequencies of the *syn* and *anti* ground-state isomers and the tunneling and torsional transition states (TS) of 5-HOTrOH. Figure 1 presents the molecule and the atomic numbering scheme used throughout this work. The calculations have been carried out at the Hartree-Fock (HF) and second-order Moller-Plesset (MP2) levels of theory.<sup>16</sup> For comparison, calculations of the  $C_s$  minimum and  $C_{2v}$  TS structures of tropolone have also been conducted at the same levels of theory. These extend the results of Bock and Redington.<sup>15</sup> In Sec. III the *ab initio* results are used to define initial projections along the intrinsic<sup>17</sup> and direct reaction coordinate pathways and to determine the overlap of the normal modes with these reaction coordinates. Section IV applies the method first to tropolone and then to 5-HOTrOH. Because the *ab initio* calculations map out the ground-state surface, their application to *syn-anti* mixing in the  $S_1$  state must be taken with some caution. Nevertheless, the experimental work of paper I show that the  $S_0$  vibrations provide a reasonable guide to the vi-

<sup>a)</sup> Authors to whom correspondence should be addressed.

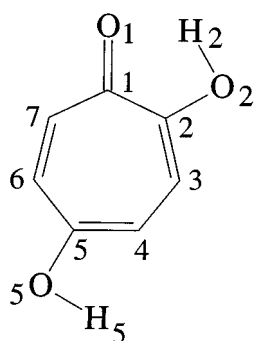


FIG. 1. Atomic numbering scheme for 5-hydroxytropolone used throughout the paper.

brations in the  $S_1$  state. Application of the method to 5-HOTrOH leads us to identify a candidate for the promoter mode W, an in-plane mode with calculated frequency of  $348\text{ cm}^{-1}$  which has unusually large overlap with the intrinsic and direct reaction coordinates for the H-atom tunneling isomerization coordinate.

## II. AB INITIO CALCULATIONS AND THE GROUND-STATE REACTION SURFACE

The *syn-anti* photoisomerization in 5-HOTrOH can occur either by 2-OH H-atom tunneling or by torsion of the 5-OH group through  $180\text{ deg}$ . The *ab initio* calculations on 5-HOTrOH focus on the *syn* and *anti* minima, the H-atom tunneling and 5-OH torsional transition states, and the H-atom/5-OH second-order saddle point across which *syn/syn* or *anti/anti* tunneling can occur. These structures and their positions in the tunneling-torsion two-dimensional potential energy surface are shown in Fig. 2. Note that motion along either the tunneling or 5-OH torsional coordinates induces *syn-anti* isomerization between inequivalent minima. Coupled motion along both coordinates (i.e., along the diagonal) connects equivalent minima. The geometry optimizations for these structures were carried out at both the HF and MP2 levels of theory using the 6-31G\*\* basis set,<sup>17</sup> which includes one set of *d* polarization functions on the carbon and oxygen atoms and one set of *p* polarization functions on the hydrogen atoms. Analogous calculations on the minimum energy and TS structures of tropolone were carried out using the same basis sets for comparison.

With the exception of the 5-OH torsional TS ( $C_1$ ) all of the geometry optimizations were carried out with  $C_s$  symmetry constraints. For the *anti* isomer, the frequency calculations reveal that the HF/6-31G\*\*  $C_s$  optimized structure is not a minimum. In this case, the structure was reoptimized with the symmetry constraint removed. The HF/6-31G\*\* and MP2/6-31G\*\* optimized geometries were used for additional single-point calculations with several larger basis sets, including the 6-311G\*\* and the 6-31++G\*\* basis sets.<sup>18,19</sup> The latter includes an additional set of diffuse *s*- and *p*-type functions on carbon and oxygen atoms and a set of diffuse *s*-type functions on the hydrogen atoms. All calculations were carried out with the GAUSSIAN92 program.<sup>20</sup>

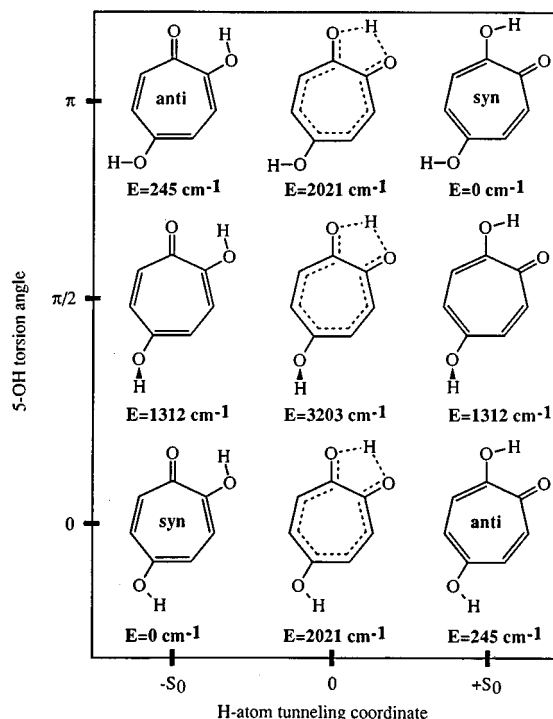


FIG. 2. Structures and positions on the H-atom tunneling/5-OH torsional two-dimensional potential energy surface. Relative energies of the various stationary states computed at the MP2/6-31G\*\* level (in  $\text{cm}^{-1}$ ) are included.

Harmonic vibrational frequencies were obtained for all structures at the HF/6-31G\*\* and MP2/6-31G\*\* levels. Similar calculations for the TS structures for 2-OH tunneling and 5-OH torsion gave a single imaginary frequency in each case. Vibrational frequency calculations for the assumed second-order saddle point at the HF/6-31G\*\* level gave only one imaginary frequency. However, the potential energy surface is very flat over 5-OH torsional angles of  $85\text{--}95\text{ deg}$ . At the MP2/6-31G\*\* level, two imaginary frequencies were obtained, thereby establishing the structure as a second-order saddle point.

Table I lists the HF/6-31G\*\* and MP2/6-31G\*\* optimized bond lengths and bond angles for all of the structures studied here. At the HF/6-31G\*\* level, there is significant bond alternation within the tropolone ring for all of the minima and TS structures. However, at the MP2/6-31G\*\* level, bond alternation is much smaller (i.e., the homoaromatic tropolone ring is more delocalized). Moreover, the MP2/6-31G\*\* optimized geometry for tropolone is in much better agreement with the geometry obtained from crystallographic data obtained for the tropolone dimer.<sup>21</sup> For this reason, we select the MP2/6-31G\*\* geometries as the most physically meaningful for these species.

The total and relative energies for the minima and transition states of tropolone and 5-HOTrOH at the HF and various MP2 levels are listed in Table II. Several conclusions about the ground-state reaction surface can be drawn from the results of the calculations.

First, the calculations predict that the *syn* conformer is more stable than the *anti* conformer. At the HF level, their

TABLE I. HF/6-31G\*\* and MP2/6-31G\*\* optimized bond lengths (Å) and bond angles (deg) for tropolone and 5-hydroxytropolone.<sup>a</sup>

Parameter <sup>c</sup>	5-Hydroxytropolone				Tropolone <sup>b</sup>			
	Syn	Anti	5-OH torsional TS <sup>d</sup>	H-atom tunneling TS	Second-order saddle point	Ground state	H-atom tunneling TS	
$r(\text{C}_1\text{C}_2)$	1.4746 (1.4663)	1.4716 (1.4647)	1.4814 (1.4703)	1.4702 (1.4652)	1.4813 (1.4696)	1.4871 (1.4725)	1.4898 (1.4726)	
$r(\text{C}_2\text{C}_3)$	1.3424 (1.3844)	1.3452 (1.3880)	1.3440 (1.3850)	1.3840 (1.4065)	1.3869 (1.4065)	1.3452 (1.3830)	1.3863 (1.4057)	
$r(\text{C}_3\text{C}_4)$	1.4336 (1.4056)	1.4288 (1.4002)	1.4321 (1.4054)	1.3890 (1.3901)	1.3847 (1.3898)	1.4316 (1.4068)	1.3858 (1.3915)	
$r(\text{C}_4\text{C}_5)$	1.3431 (1.3875)	1.3447 (1.3903)	1.3422 (1.3850)	1.3805 (1.4038)	1.3855 (1.4010)	1.3452 (1.3821)	1.3863 (1.3991)	
$r(\text{C}_5\text{C}_6)$	1.4407 (1.4167)	1.4370 (1.4140)	1.4370 (1.4153)	1.3924 (1.4037)	1.3855 (1.4010)	1.4332 (1.4130)	1.3863 (1.3991)	
$r(\text{C}_6\text{C}_7)$	1.3385 (1.3748)	1.3412 (1.3788)	1.3421 (1.3768)	1.3776 (1.3874)	1.3847 (1.3898)	1.3448 (1.3768)	1.3858 (1.3915)	
$r(\text{C}_7\text{C}_1)$	1.4597 (1.4398)	1.4574 (1.4370)	1.4547 (1.4388)	1.3921 (1.4073)	1.3869 (1.4065)	1.4512 (1.4373)	1.3863 (1.4057)	
$r(\text{C}_1\text{O}_1)$	1.2116 (1.2626)	1.2128 (1.2641)	1.2117 (1.2617)	1.2661 (1.2982)	1.2642 (1.2965)	1.2122 (1.2605)	1.2627 (1.2959)	
$r(\text{C}_2\text{O}_2)$	1.3386 (1.3439)	1.3374 (1.3417)	1.3330 (1.3413)	1.2688 (1.2978)	1.2642 (1.2965)	1.3295 (1.3398)	1.2627 (1.2959)	
$r(\text{C}_5\text{O}_5)$	1.3536 (1.3740)	1.3567 (1.3741)	1.3727 (1.3958)	1.3614 (1.3732)	1.3765 (1.3957)	1.0754 (1.0832) <sup>e</sup>	1.0749 (1.0838) <sup>e</sup>	
$r(\text{C}_3\text{H})$	1.0758 (1.0844)	1.0758 (1.0844)	1.0756 (1.0844)	1.0747 (1.0842)	1.0745 (1.0841)	1.0756 (1.0838)	1.0746 (1.0841)	
$r(\text{C}_4\text{H})$	1.0778 (1.0869)	1.0749 (1.0840)	1.0756 (1.0843)	1.0788 (1.0876)	1.0765 (1.0847)	1.0766 (1.0842)	1.0774 (1.0854)	
$r(\text{C}_6\text{H})$	1.0757 (1.0846)	1.0790 (1.0880)	1.0763 (1.0849)	1.0759 (1.0844)	1.0765 (1.0847)	1.0774 (1.0849)	1.0774 (1.0854)	
$r(\text{C}_7\text{H})$	1.0751 (1.0845)	1.0751 (1.0847)	1.0751 (1.0846)	1.0747 (1.0842)	1.0745 (1.0841)	1.0751 (1.0840)	1.0746 (1.0841)	
$r(\text{O}_2\text{H}_2)$	0.9504 (0.9898)	0.9506 (0.9914)	0.9514 (0.9903)	1.2206 (1.2360)	1.2045 (1.2290)	0.9521 (0.9914)	1.2036 (1.2283)	
$r(\text{O}_5\text{H}_5)$	0.9430 (0.9663)	0.9416 (0.9654)	0.9442 (0.9659)	0.9421 (0.9658)	0.9441 (0.9660)			
$r(\text{O}_1\text{O}_2)$	2.5495 (2.5139)	2.5512 (2.5098)	2.5365 (2.5066)	2.2558 (2.3107)	2.2531 (2.3090)	2.5241 (2.4995)	2.2517 (2.3074)	
$\angle \text{C}_1\text{C}_2\text{C}_3$	128.63 (129.94)	128.66 (130.08)	128.93 (130.17)	126.87 (127.36)	127.45 (127.66)	129.27 (130.34)	127.73 (127.85)	
$\angle \text{C}_2\text{C}_3\text{C}_4$	131.14 (129.80)	131.24 (129.81)	130.52 (129.39)	128.85 (128.85)	128.17 (128.46)	129.77 (128.93)	127.62 (128.07)	
$\angle \text{C}_3\text{C}_4\text{C}_5$	129.07 (128.87)	129.22 (128.93)	129.38 (128.96)	130.74 (129.73)	130.86 (129.74)	129.63 (129.15)	130.95 (129.83)	
$\angle \text{C}_4\text{C}_5\text{C}_6$	126.75 (127.28)	126.33 (127.12)	126.78 (127.58)	126.74 (127.90)	127.03 (128.27)	127.06 (127.75)	127.40 (128.51)	
$\angle \text{C}_5\text{C}_6\text{C}_7$	130.23 (130.00)	130.51 (130.09)	130.52 (130.02)	130.63 (129.69)	130.86 (129.74)	130.58 (130.11)	130.95 (129.83)	
$\angle \text{C}_6\text{C}_7\text{C}_1$	131.17 (131.15)	131.25 (131.24)	130.75 (130.81)	128.55 (128.82)	128.17 (128.46)	130.35 (130.47)	127.62 (128.07)	
$\angle \text{C}_7\text{C}_1\text{C}_2$	123.01 (122.95)	122.79 (122.74)	123.09 (123.04)	127.63 (127.65)	127.45 (127.66)	123.35 (123.25)	127.73 (127.85)	
$\angle \text{O}_1\text{C}_1\text{C}_2$	117.10 (115.51)	117.31 (115.54)	116.50 (115.28)	108.06 (108.93)	107.77 (108.89)	115.94 (115.06)	107.56 (108.79)	
$\angle \text{O}_2\text{C}_2\text{C}_1$	112.78 (111.92)	112.81 (111.78)	112.50 (111.67)	108.05 (109.09)	107.77 (108.89)	112.23 (111.49)	107.56 (108.79)	
$\angle \text{O}_5\text{C}_5\text{C}_4$	122.08 (120.61)	116.52 (113.99)	118.77 (116.89)	119.96 (119.34)	116.45 (115.82)	117.32 (116.31) <sup>f</sup>	116.30 (115.75) <sup>f</sup>	
$\angle \text{C}_2\text{O}_2\text{H}_2$	107.46 (101.95)	107.47 (101.78)	107.49 (102.01)	92.33 (90.86)	92.96 (91.16)	107.41 (101.91)	93.15 (91.28)	
$\angle \text{C}_4\text{C}_3\text{H}$	114.86 (116.35)	114.85 (116.39)	115.25 (116.68)	116.59 (116.88)	117.12 (117.21)	115.84 (117.07)	117.61 (117.61)	
$\angle \text{C}_5\text{C}_4\text{H}$	116.68 (115.99)	115.24 (114.31)	115.45 (114.62)	115.21 (115.30)	113.78 (113.90)	116.34 (115.91)	114.83 (115.28)	
$\angle \text{C}_7\text{C}_6\text{H}$	116.72 (116.51)	114.83 (114.74)	116.26 (116.28)	115.82 (116.65)	115.36 (116.36)	115.01 (114.80)	114.23 (114.89)	
$\angle \text{C}_1\text{C}_7\text{H}$	111.48 (112.26)	111.47 (112.28)	111.66 (112.32)	114.53 (114.30)	114.71 (114.33)	111.72 (112.31)	114.77 (114.32)	

<sup>a</sup>The MP2/6-31G\*\* values are in parentheses.<sup>b</sup>The HF/6-31G\*\* values for tropolone were taken from Ref. 15.<sup>c</sup>Atomic numbering is given in Fig. 1.<sup>d</sup>At both the HF/6-31G\*\* and MP2/6-31G\*\* levels, this structure was nearly planar even though the optimizations were carried out assuming C<sub>1</sub> symmetry.<sup>e</sup>For tropolone, this value is the C<sub>5</sub>H bond length.<sup>f</sup>For tropolone, this value is the HC<sub>5</sub>C<sub>4</sub> bond angle.TABLE II. Total energy (a.u.) for tropolone and 5-hydroxytropolone.<sup>a</sup>

Structure	HF/6-31G** <sup>b</sup>		MP2/6-31G** <sup>c</sup>	
	HF/6-31G**	MP2/6-31G**	MP2/6-31G**	MP2/6-31++G**
<i>Syn</i>	-493.129 885 6 (0.0)	-494.565 372 7 (0.0)	-494.782 489 1 (0.0)	-494.601 184 5 (0.0)
<i>Anti</i>	-493.126 544 6 (733)	-494.564 258 0 (245)	-494.781 432 4 (232)	-494.600 311 0 (192)
5-OH	-493.125 734 6 (911)	-494.559 394 8 (1312)	-494.776 955 1 (1214)	-494.595 929 3 (1153)
torsional TS				
H-atom tunneling TS	-493.099 597 2 (6646)	-494.556 162 8 (2021)	-494.773 678 3 (1933)	-494.591 562 6 (2111)
Second-order saddle point	-493.098 949 3 (6788)	-494.550 774 9 (3203)	-494.768 720 2 (3021)	-494.586 760 0 (3165)
Tropolone	-418.272 247 2 (0.0)	-419.531 076 6 (0.0)	-419.706 314 5 (0.0)	-419.560 132 5 (0.0)
H-atom tunneling TS	-418.247 349 4 (5463)	-419.522 646 4 (1850)	-419.698 314 5 (1755)	-419.551 252 8 (1948)

<sup>a</sup>Relative energies (in cm<sup>-1</sup>) are in parentheses.<sup>b</sup>HF/6-31G\*\* optimized geometries.<sup>c</sup>MP2/6-31G\*\* optimized geometries.

energy difference ( $733\text{ cm}^{-1}$ ) is three times the experimental value ( $249\text{ cm}^{-1}$ ), but the MP2/6-31G\*\* calculations ( $245\text{ cm}^{-1}$ ) reproduce the experimental value quite closely. As the single-point calculations with larger basis sets indicate, the excellent agreement between MP2/6-31G\*\* and experimental energy differences is somewhat fortuitous, due to a cancellation of errors arising from the use of a modest sized basis set and the recovery of only second-order electron correlation energy.

Second, in both tropolone and 5-HOTrOH, the barrier to H-atom tunneling drops dramatically when electron correlation at the MP2 level is taken into account. This has been noted previously for tropolone<sup>15</sup> and malonaldehyde.<sup>12</sup> In their study of malonaldehyde, Frisch *et al.*<sup>12</sup> included single-point calculations of the tunneling barrier at MP3 and MP4 levels. Based on the observed trends, the authors conclude that the true barrier height is about 30% above the MP2 barrier. Using this number as a guide leads to predicted barrier heights of  $\sim 2400\text{ cm}^{-1}$  (6.8 kcal/mol) for tropolone and  $\sim 2600\text{ cm}^{-1}$  (7.4 kcal/mol) for 5-HOTrOH. Note that the calculated transition state is the minimum-energy saddle point in the potential energy surfaces, and may not represent the actual route taken by a multidimensional tunneling reaction.<sup>5</sup>

Third, the calculated barrier to 5-OH torsion in 5-HOTrOH is close to that calculated for phenol.<sup>22,23</sup> Head-Gordon and Pople<sup>22</sup> recently carried out calculations on the OH torsional barrier in phenol at both the HF/6-311G\*\* and MP2/6-311G\*\* levels of theory and obtained barriers of 900 and  $1176\text{ cm}^{-1}$ , respectively. Kim and Jordan<sup>23</sup> have recently carried out extensive calculations of this same barrier using several basis sets and inclusion of electron correlation by means of the MP4 and QCISD(T) methods. Based on their calculations, these authors conclude that phenol's OH torsional barrier is about  $1076\text{ cm}^{-1}$ . In 5-HOTrOH, the corresponding 5-OH torsional barrier height changes from 911 to  $1312\text{ cm}^{-1}$  in going between the HF/6-31G\*\* and MP2/6-31G\*\* levels, indicating a similar magnitude for the barrier to that in phenol and a similar dependence of the barrier on electron correlation. We surmise on this basis that the 5-OH torsional barrier arises largely out of the interaction of the  $p\pi$  orbital of the hydroxy oxygen atom and the  $\pi$  system in tropolone.

Fourth, at the MP2/6-31G\*\* level the energy of the second-order saddle point (relative to the minima) is roughly equal to the sum of the 5-OH torsion and 2-OH tunneling barrier heights ( $3333$  vs  $3203\text{ cm}^{-1}$ ). It thus appears that the two motions are largely decoupled from one another.

Fifth, even at the MP2 level, the barrier associated with the second-order saddle point is large enough ( $3203\text{ cm}^{-1}$ ) that *syn-syn* or *anti-anti* tunneling splittings induced by the concerted H-atom tunneling/5-OH torsion diagonal pathway (Fig. 2) would be negligible in the experiment described in paper I. However, higher resolution experiments may be able to detect these splittings, and would provide an additional test of the accuracy of the calculations.

Finally, it needs to be emphasized again that the *ab initio* calculations map out the ground-state potential energy surface of 5-HOTrOH, while the experimental results of paper I

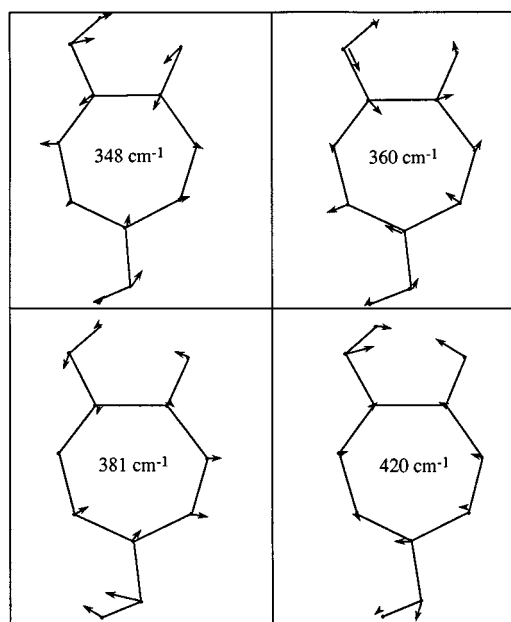


FIG. 3. Normal coordinates of several in-plane ( $a'$ ) modes in the  $300\text{--}500\text{ cm}^{-1}$  region of 5-HOTrOH. These modes are potential candidates for the promoter mode W found in the experimental study. The vectors represent the mass-weighted atomic displacements of each atom.

focus primary attention on the molecule's first excited singlet state. Nevertheless, paper I has shown a reasonable one-for-one correspondence between the  $S_0$  and  $S_1$  vibrations, so that an exploration of mode specificity in  $S_0$  can shed some light on isomerization in  $S_1$ .

### III. *AB INITIO* CALCULATIONS AND MODE SELECTIVITY: MAPPING NORMAL COORDINATES ONTO REACTION COORDINATES

#### A. General considerations

At the MP2/6-31G\*\* level, four in-plane vibrations of the *syn* and *anti* conformers are calculated to have frequencies in the  $300\text{--}500\text{ cm}^{-1}$  region, and are thereby potential candidates for the promoter mode W in 5-HOTrOH. The mass-weighted atomic displacements associated with these MP2 normal modes are shown in Fig. 3. A qualitative comparison of the vibrational modes with the *syn*-to-TS geometry change points to the 348 and  $420\text{ cm}^{-1}$  modes as vibrations which move the molecule toward the tunneling transition state. Both vibrations move the oxygen atoms toward one another and the tunneling H atom toward the acceptor oxygen, motions one would expect to enhance H-atom tunneling. However, in general it is hard to evaluate the importance of carbon skeletal motion relative to motion by the oxygens and tunneling H atom. It is also difficult to compare one mode to another or to eliminate modes as candidates for enhanced *syn-anti* coupling.

In 5-HOTrOH there is the additional complication that two *syn-anti* isomerization reaction coordinates exist: H-atom tunneling and 5-OH torsion. It is our expectation that the H-atom tunneling coordinate is the most effective route for isomerization in the  $S_1$  state of 5-HOTrOH and thus deserves primary attention. The experimental work on

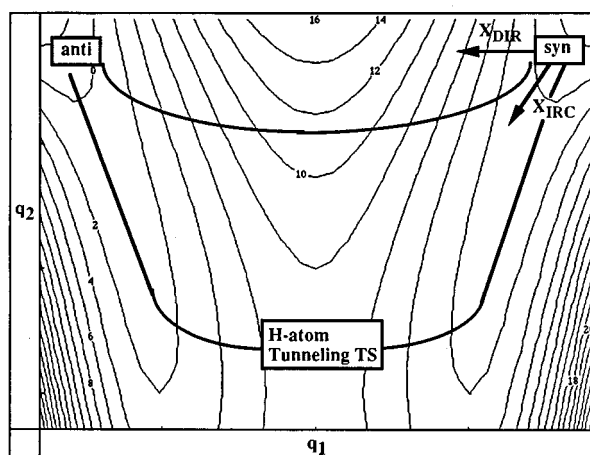


FIG. 4. Schematic two-dimensional potential energy surface for the H-atom tunneling isomerization in 5-HOTrOH. The scale on the diagram approximates the potential energy in kcal/mol. The  $q_1$  coordinate is a mass-weighted coordinate related to the H-atom position ( $q_1=0$  is when H is midway between the two oxygens). The  $q_2$  coordinate is related to the O–O distance. See Ref. 5 for details. The trajectory through the H-atom tunneling TS is the intrinsic reaction coordinate (IRC) with its low barrier and extensive oxygen atom motion. The other trajectory is a more typical reaction trajectory which cuts the corner by tunneling through a higher barrier with less oxygen–atom motion.  $X_{\text{DIR}}$  and  $X_{\text{IRC}}$  are the initial projections along the intrinsic and direct reaction pathways as defined in the text.

tropolone<sup>1–4</sup> has shown that the H-atom tunneling splitting increases by about a factor of 20 upon electronic excitation due to a decrease in the barrier to H-atom tunneling in the  $S_1$  state. Large, mode-specific changes in the H-atom tunneling splitting have been observed in  $S_1$  tropolone.<sup>1–4</sup> By contrast, if the analogy with phenol carries over to the  $S_1$  state, the barrier to 5-OH torsion in 5-HOTrOH should increase by about a factor of 4<sup>24</sup> upon  $\pi \rightarrow \pi^*$  excitation, making it unlikely that the OH torsion will be effective in promoting *syn*–*anti* coupling at low energies.

Even if one considers only H-atom tunneling, the proper choice of reaction coordinate must be resolved. To see this, Fig. 4 presents a schematic, mass-weighted 2D potential energy surface for H-atom tunneling similar to that used in past studies on malonaldehyde.<sup>5,6,13</sup> In Fig. 3, the coordinates  $q_1$  and  $q_2$  can be loosely associated with the H-atom distance from the O–O midpoint ( $q_1=0$  places the H equidistant between the two oxygens) and the O–O distance (relative to that at the saddle point), respectively. The other  $3N-8$  vibrational coordinates are then treated adiabatically to produce an effective potential energy surface for reaction.

As is apparent from Fig. 4, the reaction pathway on this heavy–light–heavy surface can be thought of in one of two limiting cases. The intrinsic reaction coordinate (IRC) first put forward by Fukui<sup>16</sup> is a steepest descent path in the mass-weighted Cartesian displacements from the saddle point into reactant and product valleys. As seen in the figure, this pathway is a highly curved, minimum-energy pathway involving extensive heavy-atom motion.<sup>5</sup> In this limit, tunneling through the barrier occurs only at the most favorable heavy-atom geometries. Alternatively, the direct, minimum-distance reaction path involves primarily H-atom motion through a

much higher tunneling barrier. Here, only heavy atom motion which moves reactants directly to products promotes reaction. In this limit, the transition state energies and structures calculated by the *ab initio* calculations would be less relevant since the molecule never samples this region of the potential energy surface in the tunneling reaction. The previous studies on model systems such as malonaldehyde<sup>5</sup> have concluded that the actual reaction path is a compromise between these two extremes, i.e., the intrinsic and direct reaction coordinates overemphasize and underemphasize heavy atom motion, respectively.

Thus, in seeking a quantitative measure of the ability of a given normal mode to promote the tunneling reaction, we wish to consider the overlap of the normal coordinates with both intrinsic and direct reaction coordinates, recognizing that the actual path for the tunneling reaction is likely a compromise between the two.<sup>5</sup> Our expectation is that heavy-atom motion along the intrinsic path will be most effective in reducing the effective barrier to H-atom tunneling.

## B. Methodology

The *ab initio* calculations provide reactant, product, and TS structures as well as the atomic displacements associated with the normal coordinates for tropolone and 5-HOTrOH. The  $3N-6$  normal coordinates form an orthonormal set of mass-weighted vibrational displacements, i.e., following mass weighting of the atomic displacements from the calculations (as the square root of the mass of each atom),

$$Q_i \cdot Q_j = \delta_{ij} \text{ for all } i, j. \quad (1)$$

Furthermore, as long as we are careful to exclude internal motions which generate angular momentum, the normal coordinates form a complete basis set for mass-weighted, internal nuclear displacements  $X$ . Thus we can write  $X$  as a linear combination of the normal coordinates:

$$X = \sum_{i=1}^{3N-6} c_i \cdot Q_i, \text{ where } c_i = X \cdot Q_i. \quad (2)$$

Initial projections of the intrinsic and direct reaction coordinates can thus be defined as mass-weighted, normalized displacement vectors located on each atom, similar in form to the normal coordinates. The initial projection of the intrinsic reaction coordinate ( $X_{\text{IRC}}$ ) is defined as

$$X_{\text{IRC}} = N_{\text{IRC}} [\sqrt{m_1}(\mathbf{r}_1^{\text{TS}} - \mathbf{r}_1^{\text{syn}}), \sqrt{m_2}(\mathbf{r}_2^{\text{TS}} - \mathbf{r}_2^{\text{syn}}), \dots, \sqrt{m_N}(\mathbf{r}_N^{\text{TS}} - \mathbf{r}_N^{\text{syn}})], \quad (3)$$

where  $\mathbf{r}_i^{\text{TS}}$  is the position of atom  $i$  with mass  $m_i$  in the transition state structure,  $\mathbf{r}_i^{\text{syn}}$  is the position of atom  $i$  in the *syn* equilibrium structure, and  $N_{\text{IRC}}$  is a normalization constant. Similarly, the initial projection of the direct reaction coordinate ( $X_{\text{DIR}}$ ) is taken to be

$$X_{\text{DIR}} = N_{\text{DIR}} [\sqrt{m_1}(\mathbf{r}_1^{\text{anti}} - \mathbf{r}_1^{\text{syn}}), \sqrt{m_2}(\mathbf{r}_2^{\text{anti}} - \mathbf{r}_2^{\text{syn}}), \dots, \sqrt{m_N}(\mathbf{r}_N^{\text{anti}} - \mathbf{r}_N^{\text{syn}})] \quad (4)$$

with  $N_{\text{DIR}}$  a normalization constant.

To implement these definitions,<sup>25</sup> the center-of-mass of a given minimum energy or TS structure is located and set at the origin of the Cartesian axis system. All of the *ab initio* structures are then rotated into a reference configuration. In tropolone and 5-HOTrOH, the reference configuration places the seven-membered ring in the  $x$ - $y$  plane with the positive  $y$  axis bisecting the  $C_1$ - $C_2$  bond (Fig. 1).

Simple application of Eqs. (3) and (4) with all structures placed in their reference configurations leads to spurious results, because the structural change which occurs in going from reactant to TS or product may incorporate a component of rotation.<sup>26</sup> In order to remove this component of rotation, the TS or product structures must be placed in an orientation relative to the *syn* conformer which generates no angular momentum. For instance, for the direct reaction coordinate, one compares the *anti* (product) structure to the *syn* structure. The proper orientation for the *anti* structure,  $\mathbf{r}_i^a$ , must be rotated from its reference orientation  $\mathbf{r}_i^{a,0}$  by an angle  $\phi$  in order to make  $L_{\text{DIR}}$  zero, where

$$\mathbf{L}_{\text{DIR}} = \sum_{i=1}^N m_i \mathbf{r}_i \times \dot{\mathbf{r}}_i = 0. \quad (5)$$

In Eq. (5),  $\dot{\mathbf{r}}_i = \Delta \mathbf{r}_i = \mathbf{r}_i^{\text{anti}} - \mathbf{r}_i^{\text{syn}}$  is the displacement along the direct reaction coordinate per unit time.<sup>26</sup> For both direct and intrinsic H-atom tunneling coordinates, the angular momentum which must be nulled is about the out-of-plane ( $z$ ) axis. Thus,

$$L_z = \sum_{i=1}^N m_i [x_i^s (y_i^a - y_i^s) - y_i^s (x_i^a - x_i^s)], \quad (6)$$

where

$$\begin{aligned} x_i^a &= x_i^{a,0} \cos(\phi) - y_i^{a,0} \sin(\phi), \\ y_i^a &= y_i^{a,0} \cos(\phi) + x_i^{a,0} \sin(\phi). \end{aligned} \quad (7)$$

Upon determining the angle  $\phi$ , the product or TS structure is rotated by  $\phi$  (typically  $< 1$  deg) from its reference configuration, and the intrinsic and direct reaction coordinates are formed according to Eqs. (3) and (4), respectively.

A total of six reaction coordinates have been calculated: the intrinsic and direct H-atom tunneling coordinates in tropolone and in 5-HOTrOH, and the intrinsic and direct 5-OH torsion reaction coordinates in 5-HOTrOH. These are shown pictorially in Fig. 5 and are listed in Table III.

To determine the overlap of the normal coordinates with the reaction coordinates, the normal coordinate atomic displacements are considered in the reference (reactant) configuration. After mass-weighting and normalization of the normal coordinates, the overlap is calculated using Eq. (2). The normal coordinate/reaction coordinate overlap coefficients are collected in Table IV for tropolone and in Table V for 5-HOTrOH. In the case of tropolone, all in-plane vibrations have been included in the table, while for 5-HOTrOH, only those vibrations most relevant to the spectroscopy of paper I are shown. An overlap coefficient of 1 would indicate that that normal mode projects directly along the reaction

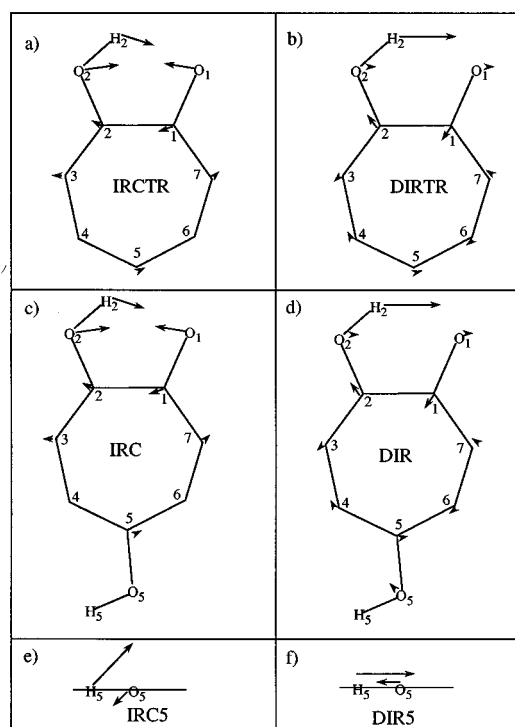


FIG. 5. Mass-weighted, normalized displacement vectors representing initial projections along the intrinsic and direct reaction pathways in tropolone and 5-HOTrOH. (a),(b) The designations IRCTR and DIRTR represent the intrinsic and direct initial projections for H-atom tunneling in tropolone. (c),(d) IRC and DIR are the corresponding projections in 5-HOTrOH. (e),(f) IRC5 and DIR5 are the intrinsic and direct projections along the 5-OH torsional reaction coordinate in 5-HOTrOH. Only the 5-OH group is shown since it carries the only significant motion along the IRC5 and DIR5 coordinates.

coordinate, while a coefficient of 0 indicates that the vibrational motion is orthogonal to the reaction coordinate.

## IV. DISCUSSION

### A. The form of the reaction coordinates

The reaction coordinate projections presented in Fig. 5 and Table III contain several interesting features which deserve discussion.

First, the form of the intrinsic and direct H-atom tunneling coordinates are almost identical in tropolone (IRCTR, DIRTR) and 5-HOTrOH (IRC, DIR), especially with respect to the five-membered ring formed by  $O_1$ ,  $C_1$ ,  $C_2$ ,  $O_2$ , and  $H_2$  in which H-atom tunneling occurs. The coefficient of overlap between IRCTR and IRC is 0.998, while that between DIRTR and DIR is 0.940. This is not unexpected, since 5-OH substitution should not induce major changes in the H-atom tunneling reaction coordinate.

Second, both the intrinsic and direct H-atom tunneling reaction coordinates have dominant weighting in motion of the  $O_1$ - $H_2$ - $O_2$  triad. In tropolone, the contribution to the normalized reaction coordinate from these three atoms has magnitude:

$$\begin{aligned} |c_{\text{triad}}| &= (c_{O_1}^2 + c_{H_2}^2 + c_{O_2}^2)^{1/2} \\ &= 0.946 \text{ for IRCTR and } 0.918 \text{ for DIRTR.} \end{aligned}$$

TABLE III. Mass-weighted initial projections along the intrinsic and direct reaction pathways for tropolone and 5-HOTrOH.

	Tropolone H-atom tunneling				5-HOTrOH H-atom tunneling				5-HOTrOH 5-OH torsion				
	IRCTR		DIRTR		IRC		DIR		IRC5			DIR	
	x	y	x	y	x	y	x	y	x	y	z	x	y
O <sub>1</sub> <sup>a</sup>	-0.479	-0.076	0.076	-0.009	-0.499	0.084	0.024	0.032	-0.015	0.016	0.072	-0.005	0.020
O <sub>2</sub>	0.524	0.062	0.076	-0.023	0.513	0.041	0.041	-0.025	0.009	-0.013	0.033	0.005	-0.016
H <sub>2</sub>	0.591	-0.177	0.911	0.016	0.581	-0.185	0.889	0.008	0.002	-0.004	0.015	0.002	-0.003
C <sub>1</sub>	-0.083	-0.220	-0.121	-0.218	-0.093	-0.217	-0.138	-0.193	0.010	0.007	0.018	0.006	0.010
C <sub>2</sub>	-0.096	0.039	-0.133	0.203	-0.096	0.028	-0.137	0.194	0.000	-0.006	0.003	0.010	-0.006
C <sub>3</sub>	-0.133	-0.062	-0.078	-0.059	-0.123	-0.070	-0.060	-0.079	-0.004	-0.004	-0.040	0.012	-0.017
C <sub>4</sub>	-0.029	0.038	-0.038	0.068	-0.006	0.027	0.025	-0.163	0.019	0.002	-0.052	0.018	-0.005
C <sub>5</sub>	0.061	0.052	0.055	0.018	0.078	0.040	0.100	-0.003	0.020	0.021	-0.023	0.026	-0.002
C <sub>6</sub>	0.021	-0.008	-0.033	-0.047	0.036	-0.002	0.007	0.167	0.018	0.016	-0.065	0.015	0.008
C <sub>7</sub>	0.038	0.057	-0.080	0.061	0.034	0.055	-0.070	0.077	0.024	0.021	-0.49	0.007	0.017
H <sub>3</sub>	-0.042	-0.032	-0.025	0.030	-0.039	-0.038	-0.022	-0.043	-0.001	-0.002	-0.018	0.003	-0.006
H <sub>4</sub>	0.008	-0.011	-0.003	0.010	0.014	-0.003	0.014	-0.003	0.023	-0.017	-0.030	0.019	-0.15
O <sub>5</sub>					-0.007	0.042	-0.040	-0.015	-0.238	-0.057	-0.214	-0.328	-0.013
H <sub>5</sub>	0.009	0.025	-0.026	0.029	-0.007	0.023	-0.019	0.019	0.640	0.028	0.676	0.942	0.026
H <sub>6</sub>	0.015	0.014	0.007	0.007	0.010	-0.000	0.015	0.007	0.007	0.007	-0.041	0.019	0.018
H <sub>7</sub>	0.005	-0.005	-0.003	-0.001	0.007	0.026	-0.025	0.041	0.006	0.009	-0.025	0.002	0.006

<sup>a</sup>Atomic numbering is given in Fig. 1.

This result is initially surprising, because formally all of the carbon-carbon bonds except C<sub>1</sub>-C<sub>2</sub> are changing bond order upon reaction. However, the MP2 calculations predict only small alternations in the C-C bond lengths around the ring, resulting in only small carbon-atom motion in moving to the TS or product. If the calculations at the HF level (Table I) were used in forming the reaction coordinates, significantly greater contributions from the ring would result. Clearly the usefulness of the present method depends critically on the accuracy of the *ab initio* calculations on which they are built.

One consequence of the heavy weighting of the reaction coordinates toward motion of the O<sub>1</sub>-H<sub>2</sub>-O<sub>2</sub> triad is that the coefficient of overlap of a given normal coordinate with the intrinsic and direct reaction coordinates is especially sensitive to the direction and magnitude of vibrational amplitude on these three atoms.

Third, as expected, the direct reaction coordinate projection weights the tunneling H-atom motion (with magnitude for the H<sub>2</sub> vector of  $|c_{H_2}|=0.911$ ) much more heavily than O-atom motions ( $|c_{O_1}|=0.076$ ,  $|c_{O_2}|=0.079$ ), while the H-atom ( $|c_{H_2}|=0.617$ ) and O-atom contributions ( $|c_{O_1}|=0.485$ ,  $|c_{O_2}|=0.528$ ) are comparable in the intrinsic reaction coordinate projection.

Fourth, the direct and intrinsic coordinates differ in the phase of motion of the oxygen atoms. As shown in Fig. 5, the intrinsic reaction coordinate involves a symmetric wagging of the two oxygen atoms; i.e., in approaching the TS, the two oxygen atoms are drawn together, as one would expect. By comparison, in the final product structure, the oxygen atom receiving the hydrogen atom relaxes back to a geometry in which it is pushed away from the donating oxygen. Consequently, the direct coordinate has a component of asymmetric wag of the oxygens, with opposite phase to the intrinsic coordinate. This difference can produce significantly different coefficients of overlap of a given normal coordinate be-

tween IRC and DIR, depending on the relative phase of oxygen motion for the vibration.

Fifth, not surprisingly, the intrinsic 5-OH torsion reaction coordinate (IRC5) is dominated almost entirely by 5-OH hydrogen atom motion, flanked by a small amount of 5-OH oxygen motion which accompanies internal rotation of the OH. The displacement of the *syn* structure toward the perpendicular transition state incorporates some in-plane character in  $X_{IRC}(5\text{-OH torsion})$ . As a result, IRC5 is not accurately reflecting the initial motion of the 5-OH torsion (when treated as a one-dimensional internal rotation), which would be purely out-of-plane. This is a limitation of the method, which fails to give an accurate initial projection of the intrinsic or direct reaction coordinates in cases where these coordinates follow highly curved pathways.

## B. The coefficients of overlap of the normal coordinates with the reaction coordinates

### 1. Tropolone

The coefficients of overlap listed in Table IV include all 27 in-plane modes of tropolone. In tropolone, both intrinsic (IRCTR) and direct (DIRTR) reaction coordinates involve only in-plane motions, so only in-plane vibrations have non-zero coefficients of overlap. Note that, as expected, the sum of the squares of the vibrational overlap coefficients equals 1.00, as it should if rotation has been properly excluded from the reaction coordinates.

In most cases, the intrinsic and direct overlap coefficients for a given vibration are of similar magnitude. However, some notable exceptions (e.g., the modes with frequencies 370 and 547 cm<sup>-1</sup>) do exist. In these cases, the normal mode has a strong symmetric or asymmetric wag of the oxygens which overlaps well with one reaction coordinate and not the other.

TABLE IV. Normal coordinate overlap with the intrinsic and direct reaction coordinates in tropolone.

MP2	Vibrational frequencies (cm <sup>-1</sup> )		Symmetry	Mode description <sup>a</sup>	<i>c</i> <sub>IRCTR(H)</sub> <sup>b</sup>	<i>c</i> <sub>DIRTR(H)</sub> <sup>c</sup>	$\frac{\Delta E(X_0^n)}{\Delta E(0_0^0)}$ <sup>d</sup>
	Expt. <i>S</i> <sub>0</sub> <sup>e</sup>	Expt. <i>S</i> <sub>1</sub> <sup>f</sup>					
105	110	39	<i>a</i> ''	<i>Q</i> 26(?)	0.000	0.000	0.37
174	177	171	<i>a</i> ''	<i>Q</i> 25(?)	0.000	0.000	0.21
356	349		<i>a</i> '		0.675	0.356	
370	359	296	<i>a</i> '	<i>Q</i> 14	0.509	0.054	1.60
446	434	414	<i>a</i> '	<i>Q</i> 13	0.390	0.166	1.68
547	551		<i>a</i> '		0.026	0.197	
706	674	640	<i>a</i> '	<i>Q</i> 12	0.013	0.056	0.89
759	742	511	<i>a</i> '	<i>Q</i> 11	0.024	0.080	0.68
900			<i>a</i> '		0.014	0.004	
990			<i>a</i> '		0.029	0.050	
1094			<i>a</i> '		0.091	0.182	
1261			<i>a</i> '		0.096	0.170	
1263			<i>a</i> '		0.094	0.194	
1302			<i>a</i> '		0.018	0.069	
1344			<i>a</i> '		0.144	0.274	
1379			<i>a</i> '		0.155	0.277	
1474			<i>a</i> '		0.076	0.145	
1497			<i>a</i> '		0.053	0.133	
1553			<i>a</i> '		0.089	0.209	
1597			<i>a</i> '		0.045	0.073	
1641			<i>a</i> '	Some C=O str.	0.032	0.053	
1677			<i>a</i> '		0.082	0.171	
1717			<i>a</i> '	Some C=O str.	0.016	0.023	
3232			<i>a</i> '		0.001	0.002	
3240			<i>a</i> '		0.004	0.008	
3257			<i>a</i> '		0.003	0.002	
3260			<i>a</i> '		0.002	0.002	
3266			<i>a</i> '		0.000	0.003	
3433			<i>a</i> '	<i>Q</i> 27, 2-OH str.	0.191	0.627	

<sup>a</sup>Vibrational numbering in tropolone is that from Ref. 28.<sup>b</sup>Coefficient of overlap between the normal mode and the intrinsic reaction coordinate in tropolone, IRCTR, as defined in Table III.<sup>c</sup>Coefficient of overlap between the normal mode and the direct reaction coordinate in tropolone, DIRTR, as defined in Table III.<sup>d</sup>Ratio of the tunneling splitting of the *S*<sub>0</sub>-*S*<sub>1</sub>*X*<sub>0</sub><sup>n</sup> transition to that at the *S*<sub>1</sub> origin. For the in-plane modes, *n*=1 while for the out-of-plane modes, *n*=2.<sup>e</sup>Taken from Ref. 15.<sup>f</sup>Taken from Ref. 4.TABLE V. Normal coordinate overlap with the intrinsic and direct reaction coordinates along H-atom tunneling and 5-OH torsion pathways in *syn* 5-hydroxytropolone.

MP2	Vibrational frequencies (cm <sup>-1</sup> )		Symmetry	Mode description	<i>c</i> <sub>IRC(H)</sub>	<i>c</i> <sub>DIR(H)</sub>	<i>c</i> <sub>IRC(5-OH)</sub>	<i>c</i> <sub>DIR(5-OH)</sub>
	Expt. <i>S</i> <sub>0</sub>							
122	97		<i>a</i> ''	<i>Q</i> 26(?)	0.000	0.000	0.108	0.000
140	128		<i>a</i> ''	<i>Q</i> 25(?)	0.000	0.000	0.014	0.000
348	336		<i>a</i> '	W	0.670	0.260	0.010	0.020
360	353		<i>a</i> '	X	0.023	0.109	0.011	0.023
381	369		<i>a</i> '	Y	0.097	0.063	0.037	0.022
420	400		<i>a</i> '	Z	0.634	0.234	0.028	0.017
464			<i>a</i> ''	5-OH torsion	0.000	0.000	0.689	0.000
602			<i>a</i> '		0.042	0.329	0.005	0.005
3484			<i>a</i> '	2-OH stretch	0.193	0.626	0.001	0.001

Very few vibrations have large overlap with the reaction coordinates. In IRCTR, only three vibrations have coefficients above 0.20, while four exceed this threshold in DIRTR. These vibrations are concentrated in the low-frequency region around 300–500  $\text{cm}^{-1}$ , and in the OH stretching mode. Not surprisingly, DIRTR, with its dominant H-atom motion, has a particularly large overlap with the OH stretching mode (0.627). The large overlaps of vibrations in the 300–500  $\text{cm}^{-1}$  region arises because of the heavy weighting of oxygen atom motion in the reaction coordinates. Vibrations which incorporate significant C–O wag are in this frequency range.

Redington<sup>14</sup> has recently analyzed the infrared spectrum of tropolone in a neon matrix. Of the 39 vibrational modes of tropolone, only three fundamentals were reported to have enhanced tunneling splittings in the vibrationally excited states:  $Q_{34}$  (CC stretch, 1306  $\text{cm}^{-1}$ ),  $Q_{31}$  (C=O stretch, 1565  $\text{cm}^{-1}$ ), and  $Q_{27}$  (O–H stretch, 3121  $\text{cm}^{-1}$ ). The vibrations in the 300–500  $\text{cm}^{-1}$  region do not show unusually large tunneling splittings. This is due to the fact that, in the ground state of tropolone, the barrier to H-atom tunneling is large enough that even with strong coupling to the reaction coordinate, tunneling splittings are still small at the low energies associated with these vibrations.

However, the first excited singlet state has a much smaller barrier to H-atom tunneling. The extensive studies of the  $S_0$ – $S_1$  spectrum of tropolone<sup>1–4</sup> have led to assignments and tunneling splittings for several prominent modes in the low-frequency region of  $S_1$ . The frequencies and Franck–Condon activities of these vibrations show a good one-to-one correspondence between the vibrations in  $S_0$  and  $S_1$ . Table IV lists the experimental ground-state and excited-state vibrational frequencies of several of these modes, and the most probable correlation with the *ab initio* calculations.

The comparison with experiment is quite encouraging. Included in Table IV is the ratio of the tunneling splitting at  $v'=1$  in  $S_1$  to that at the  $S_1$  origin [i.e.,  $\Delta E(X_0^1)/\Delta E(0_0^0)$ ]. In cases where overtones of out-of-plane vibrations are excited, the reported ratio is for the  $X_0^2$  transition. As has been noted by several authors previously,<sup>1,3,4</sup> the out-of-plane vibrations  $Q_{25}$  and  $Q_{26}$  strongly inhibit H-atom tunneling relative to the origin. Consistent with this fact,  $Q_{25}$  and  $Q_{26}$  are strictly orthogonal to both IRCTR and DIRTR. In the same way, the in-plane vibrations  $Q_{11}$  and  $Q_{12}$ , which are calculated to be nearly orthogonal to IRCTR, are seen experimentally to also inhibit tunneling. However,  $Q_{13}$  and  $Q_{14}$ , which have large overlaps with IRCTR, have tunneling splittings 60% greater than the  $S_1$  origin.

The correlation of experimental tunneling splittings with the coefficients of overlap with DIRTR is much less clear for  $Q_{11}$ – $Q_{14}$ . All four vibrations have similar sized overlaps with DIRTR, and no clear trend exists. This suggests that motion along the intrinsic reaction coordinate is more effective in promoting tunneling than motion along the direct reaction coordinate. We are thereby left with a physical picture of the vibrationally mediated tunneling reaction as a two-step process in which the vibration moves the molecule up the reactant valley toward the transition state, followed by tun-

neling through a reduced barrier into the product channel (Fig. 4).

Regarding the higher frequency modes in  $S_0$ , the match-up is less satisfying. Experimentally,<sup>14</sup> the OH stretch ( $Q_{27}$ ) splitting in  $S_0$  is large, but has not been quantitatively measured due to the weakness and breadth of the transition (the OD stretch splitting in TrOD is 15.6  $\text{cm}^{-1}$ ). Not surprisingly, this mode is also calculated to have a large overlap with the reaction coordinates, especially with DIRTR. In the case of the C–C stretch ( $Q_{34}$ ), the pair of transitions originally assigned as a tunneling doublet in the experimental study<sup>14</sup> has been reassigned<sup>15</sup> subsequently as separate combination bands. Thus, this mode can no longer be considered to enhance H-atom tunneling. Finally, the fundamental assigned to the carbonyl stretch ( $Q_{31}$ , 1565  $\text{cm}^{-1}$ ) has an estimated gas phase  $v''=1$  tunneling splitting of 16.3  $\text{cm}^{-1}$ . As Table V indicates, the present calculations show partial C=O stretch character in modes at 1641 and 1717  $\text{cm}^{-1}$ . However, neither mode shows significant overlap with the reaction coordinates. On the other hand, the 1677  $\text{cm}^{-1}$  mode, straddled in frequency by the C=O stretch bands, shows larger overlaps with the reaction coordinates. Whether the theory, *ab initio* calculation, or experiment is responsible for this discrepancy is unclear.

## 2. 5-hydroxytropolone

The primary goal of this work is to identify the promoter mode W which experiment has shown plays a major role in enhancing *syn-anti* coupling in 5-HOTrOH (paper I). This vibration is a low-frequency, in-plane vibration (335  $\text{cm}^{-1}$  in the ground state,  $\sim 310$   $\text{cm}^{-1}$  in the  $S_1$  state) in the same frequency region as  $Q_{13}$  and  $Q_{14}$  in tropolone.<sup>4</sup> Table V lists the reaction coordinate overlaps of a select group of vibrations in 5-HOTrOH, including in-plane vibrations in the 300–500  $\text{cm}^{-1}$  region which are candidates for mode W. Note that a standard scaling<sup>27</sup> of the MP2 vibrational frequencies (by 0.9427) yields frequencies for the in-plane modes in excellent one-to-one correspondence with the experimental ground-state frequencies.

The correlation between the low-frequency modes in 5-HOTrOH and tropolone is shown in Table VI as a coefficient of overlap between the vibrations. In calculating the overlap, the motion of the hydrogen in the 5 position in tropolone is compared with the motion of the 5-OH oxygen in 5-HOTrOH. For the most part, a one-to-one correspondence exists between modes in the two molecules. The notable exception is mode Y in 5-HOTrOH (381  $\text{cm}^{-1}$ ), which is a 5-OH in-plane bend with no corresponding mode in this frequency range in tropolone.

Interestingly, the strong correspondence between the other tropolone and 5-HOTrOH modes does not necessarily translate into similar overlaps with the H-atom reaction coordinates. As noted earlier, in determining overlaps with the reaction coordinates, the magnitude and direction of the atoms in the  $O_1$ –H– $O_2$  triad plays a crucial role. For example, the mode at 370  $\text{cm}^{-1}$  in tropolone has a large overlap (0.827) with the mode at 360  $\text{cm}^{-1}$  in 5-HOTrOH, yet the former has a  $c_{\text{IRC}}=0.509$  while the latter has a  $c_{\text{IRC}}$  value of

TABLE VI. Coefficients of overlap between the normal modes of tropolone and 5-hydroxytropolone.

5-HOTrOH vibrational frequencies (cm <sup>-1</sup> )		Tropolone vibrational frequencies (cm <sup>-1</sup> )				
		356	370	446	547	3484
348	W	0.836	0.366	0.180	0.103	0.000
360	X	0.485	0.827	0.165	0.065	0.000
381	Y	0.130	0.144	0.291	0.426	0.000
420	Z	0.182	0.367	0.830	0.155	0.000
602		0.018	0.019	0.080	0.869	0.000
3433		0.000	0.000	0.000	0.000	1.00

only 0.023. Inspection of these modes indicates that they differ significantly in the directions of the oxygen atoms' motion.

As with tropolone, the experimental data on *syn-anti* coupling in 5-HOTrOH focuses on the low-frequency region of the  $S_1$  state. The correspondence between the  $S_0$  and  $S_1$  vibrations is reasonably good; however, some Fermi resonance mixing is present in  $S_1$  (paper I). Despite this, the striking result of the calculation of overlap coefficients is that the mode at 348 cm<sup>-1</sup>, which closely matches the promoter mode W in frequency, has a very large overlap coefficient (0.670) with the H-atom intrinsic reaction coordinate. This normal mode is shown in Fig. 3. It is describable as a symmetric wag of the two C–O groups which brings the oxygen atoms toward one another, thereby decreasing the tunneling distance for the H atom. Also consistent with experiment is the fact that modes X and Y, which are seen experimentally to have little *syn-anti* mixing in  $S_1$ , have small coefficients of overlap with the reaction coordinates.

The only other vibration in the 300–500 cm<sup>-1</sup> frequency region with a large overlap with the reaction coordinates has a frequency of 420 cm<sup>-1</sup>. This frequency clearly does not correlate as well with W as the 348 cm<sup>-1</sup> mode. We tentatively assign the 420 cm<sup>-1</sup> mode to mode Z (experimental frequency 399 cm<sup>-1</sup>). Having made this assignment in the ground state, we are faced with the fact that in  $S_1$ , this mode does not show strong *syn-anti* mixing. The reason for this discrepancy may be the aforementioned sensitivity of the reaction coordinate coefficients to the direction of O<sub>1</sub>–H–O<sub>2</sub> motion. If mode Z in the  $S_1$  state has perturbed motion in these atoms relative to that from the  $S_0$  calculations, this would explain its lack of *syn-anti* coupling. Alternatively, the reaction coordinates themselves may need to be modified somewhat in  $S_1$  relative to the present ground-state calculations.

Finally, Table V also includes overlap coefficients for the 5-OH torsional reaction coordinate, which also could induce *syn-anti* isomerization. Note that none of the in-plane modes in the 300–500 cm<sup>-1</sup> region have significant overlap with this coordinate. This confirms that it is the H-atom tunneling coordinate, rather than the 5-OH torsional coordinate, which is primarily responsible for the *syn-anti* coupling observed in 5-HOTrOH. Obviously, the 5-OH torsional reaction coordinate (IRC5) maps very closely onto the 5-OH torsional vibration. In fact, the value of intrinsic coordinate overlap coefficient,  $c_{\text{IRC}(5\text{-OH})} = 0.689$ , is just the out-of-plane component of IRC5.

## V. CONCLUSIONS

We have presented a method which uses *ab initio* calculations of the reactant, product, and transition states of an intramolecular isomerization reaction to predict which vibrational modes hold greatest promise as mode-specific promoters of the isomerization. The method has been used to assign the promoter mode W in 5-HOTrOH as a symmetric in-plane wag of the oxygen atoms.

The method has provided a useful comparison with the experimental study of paper I. In principle, such calculations could be used as the starting point for  $n$ -dimensional subspace calculations of mode-specific effects in H-atom tunneling. This would have the advantage of facilitating a more direct connection with experimental observables than the  $n$ -dimensional calculations involving localized O<sub>1</sub>–H<sub>2</sub>–O<sub>2</sub> spatial coordinates.

A significant deficiency of the application of these methods to tropolone and 5-HOTrOH is that the calculations are ground-state calculations, while *syn-anti* mixing is most sensitively probed experimentally in the  $S_1$  state. Clearly, as algorithms for calculating excited states improve, such calculations can be carried out directly on the  $S_1$  state, and will provide much additional insight to the vibrationally mode-specific behavior observed there.

Finally, while the method may identify which modes project along the reaction coordinates, other features of the isomerization must also be taken into account in answering questions of mode specificity. For example, the energy of the vibrations relative to the barrier to tunneling will determine the efficiency of tunneling. In addition, processes such as Fermi resonance (at low energies) and IVR (at higher energies) will mask the mode-specific effects if such mode mixing is efficient.

## ACKNOWLEDGMENTS

We thank Professor R. L. Redington for providing the HF/6-31G\*\* optimized geometry of the tropolone TS. The authors thank Professor J. Michl for pointing out the need to ensure that the reaction coordinate projections contain no component of rotation. T.S.Z. acknowledges a grant from the Petroleum Research Fund, administered by the American Chemical Society, for support of this work, and K.D.J. acknowledges the support of the National Science Foundation through Award No. CHE9121306. Some of the calculations were carried out on the Cray C90 at the Pittsburgh Supercomputing Center.

## SUPPLEMENTARY MATERIAL AVAILABLE

Optimized geometries obtained at the HF/6-31G\*\* and MP2/6-31G\*\* levels of theory for the 5-OH torsional TS and the second-order saddle point for 5-HOTrOH are available in Z-matrix format. Harmonic vibrational frequencies obtained at the HF/6-31G\*\* and MP2/6-31G\*\* levels for all of the structures studied here are also available. This material is contained in many libraries on microfiche, immediately follows this article in the microfilm version of the journal, and can be ordered from the APS; see any current masthead page for ordering information.

- <sup>1</sup>R. L. Redington, Y. Chen, G. J. Scherer, and R. W. Field, *J. Chem. Phys.* **88**, 627 (1988); R. L. Redington, *ibid.* **92**, 6447 (1990); R. L. Redington and C. W. Bock, *J. Phys. Chem.* **95**, 10 284 (1991).
- <sup>2</sup>Y. Tomioka, M. Ito, and N. Mikami, *J. Phys. Chem.* **87**, 4401 (1983); R. Rosetti and L. E. Brus, *J. Chem. Phys.* **73**, 1546 (1980).
- <sup>3</sup>A. C. P. Alves, J. M. Hollas, H. Musa, and T. Ridley, *J. Mol. Spectrosc.* **109**, 99 (1985).
- <sup>4</sup>H. Sekiya, Y. Nagashima, and Y. Nishimura, *J. Chem. Phys.* **92**, 5761 (1990).
- <sup>5</sup>See N. Shida, P. F. Barbara, and J. E. Almlof, *J. Chem. Phys.* **91**, 4061 (1989) for an excellent review of the field as of 1989.
- <sup>6</sup>T. D. Sewell and D. L. Thompson, *Chem. Phys. Lett.* **193**, 347 (1992).
- <sup>7</sup>T. Chiavassa, P. Roubin, L. Pizzala, P. Verlaque, A. Allouche, and F. Marinelli, *J. Phys. Chem.* **96**, 10 659 (1992).
- <sup>8</sup>J. R. de la Vega, *Acc. Chem. Res.* **15**, 185 (1982).
- <sup>9</sup>J. Bicerano, H. F. Schaefer III, and W. H. Miller, *J. Am. Chem. Soc.* **105**, 2550 (1983).
- <sup>10</sup>C. G. Truhlar, A. d. Isaacson, and B. C. Garrett, *Theory of Chemical Reaction Dynamics*, edited by M. Baer (Chemical Rubber, Boca Raton, 1985), Vols. 1 and 2.
- <sup>11</sup>T. Carrington and W. H. Miller, *J. Chem. Phys.* **84**, 4364 (1986).
- <sup>12</sup>M. J. Frisch, A. C. Scheiner, H. F. Schaefer III, and J. S. Binkley, *J. Chem. Phys.* **82**, 4194 (1985); J. S. Binkley and M. J. Frisch, *Chem. Phys. Lett.* **126**, 1 (1986).
- <sup>13</sup>J. S. Hutchinson, *J. Phys. Chem.* **91**, 4495 (1987).
- <sup>14</sup>R. L. Redington, *J. Chem. Phys.* **92**, 6447 (1990).
- <sup>15</sup>R. L. Redington and C. W. Bock, *J. Phys. Chem.* **95**, 10 284 (1991).
- <sup>16</sup>See K. Fukui, *Acc. Chem. Res.* **14**, 368 (1981), and references therein.
- <sup>17</sup>(a) J. S. Binkley, J. A. Pople, and W. J. Hehre, *J. Am. Chem. Soc.* **102**, 939 (1980); (b) W. J. Hehre, R. Ditchfield, and J. A. Pople, *J. Chem. Phys.* **56**, 2257 (1972); (c) R. Krishnan, M. J. Frisch, and J. A. Pople, *ibid.* **72**, 4244 (1980).
- <sup>18</sup>R. Krishnan, J. S. Binkley, R. Seeger, and J. A. Pople, *J. Chem. Phys.* **72**, 650 (1980).
- <sup>19</sup>(a) T. Clark, J. Chandrasekhar, G. W. Spitznagel, and P. v. R. Schleyer, *J. Comput. Chem.* **4**, 294 (1983); (b) M. J. Frisch, J. A. Pople, and J. S. Binkley, *J. Chem. Phys.* **80**, 3265 (1984).
- <sup>20</sup>GAUSSIAN92: M. J. Frisch, M. Head-Gordon, G. W. Trucks, P. M. Gill, M. W. Wong, J. B. Foresman, B. G. Johnson, H. B. Schlegel, E. S. Replogle, R. Gomberts, J. L. Andres, K. Raghavachari, M. A. Robb, J. S. Binkley, C. Gonzalez, D. J. Defrees, D. J. Fox, J. Baker, R. L. Martin, and J. A. Pople (Gaussian, Pittsburgh, PA, 1992).
- <sup>21</sup>H. Shimanouchi and Y. Sasada, *Acta Crystallogr. Sect. B* **29**, 81 (1973).
- <sup>22</sup>M. Head-Gordon and J. A. Pople, *J. Phys. Chem.* **97**, 1147 (1993).
- <sup>23</sup>K. Kim and K. D. Jordan, *Chem. Phys. Lett.* **218**, 261 (1994).
- <sup>24</sup>H. D. Bist, J. C. D. Brand, and D. R. Williams, *J. Mol. Spectrosc.* **24**, 402 (1967).
- <sup>25</sup>A. MATHCAD program specific to tropolone and 5-HOTrOH has been written for this purpose.
- <sup>26</sup>B. R. Arnold, V. Balaji, J. W. Downing, J. G. Radziszewski, J. J. Fisher, and J. Michl, *J. Am. Chem. Soc.* **113**, 2910 (1991).
- <sup>27</sup>J. A. Pople, A. P. Scott, M. W. Wong, and L. Radom, *Isr. J. Chem.* **33**, 345 (1993).
- <sup>28</sup>R. L. Redington and T. E. Redington, *J. Mol. Spectrosc.* **78**, 229 (1979).